Estimation of Tsunami-Inundated Areas in Asahi City, Chiba Prefecture, after the 2011 Tohoku-Oki Earthquake

Yoshihisa Maruyama,[a) M.EERI, Ken Kitamura,[a) and Fumio Yamazaki[a) M.EERI

The 2011 off the Pacific coast of Tohoku-oki earthquake triggered an extremely large tsunami. The authors conducted a field survey in Asahi City, Chiba Prefecture, after the occurrence of the earthquake. Although located farther away from the source region of the earthquake, there was still significant damage in this area. Tsunami-inundated areas in Asahi City were identified from the map developed by disaster relief volunteers and the satellite images captured after the event. Polygons to demonstrate the tsunami-inundated areas were developed in the geographic information system. The authors compared the identified affected areas with the existing tsunami hazard map of Asahi City. The relationship between the tsunami-inundated areas and the locations of seawalls and tide-prevention forests was evaluated. In addition, a numerical simulation of tsunami propagation was performed and the ratio of totally collapsed buildings to the total number of buildings, that is, damage ratio, in terms of the estimated inundation depths was evaluated. [DOI: 10.1193/1.4000123]

INTRODUCTION

The 2011 Tohoku-oki earthquake, which occurred on 11 March 2011, triggered an extremely large tsunami. The run-up reached a maximum height of 40.4 m in Tohoku region (The 2011 Tohoku Earthquake Tsunami Joint Survey Group 2011). The Japanese National Police Agency (2011) confirmed more than 15,000 deaths and 3,400 people missing. According to the Cabinet Office (2011), 92.4% of the fatalities in Iwate, Miyagi, and Fukushima Prefectures resulted from drowning.

The tsunami also affected Chiba Prefecture, which is located farther away from the earthquake source region, compared to the more severely affected areas in Iwate, Miyage and Fukushima prefectures. With 13 fatalities in Asahi City (Figure 1) and two people reported still missing, the eastern part of the prefecture was severely affected. In Asahi City, 336 family units collapsed as a result of this event (Asahi City 2011). These buildings were mainly affected by the tsunami, and liquefaction. The people in Asahi City suffered from both the tsunami and liquefaction, although they were away from the most severely affected areas in Tohoku.

Figure 2 shows the distribution of totally collapsed buildings by the tsunami in Asahi City. The dataset was compiled by the city and the number of totally collapsed buildings was

[a) Graduate School of Engineering, Chiba University, 1-33 Yayoi-cho, Inage-ku, Chiba 263-8522, Japan

Earthquake Spectra, Volume 29, No. S1, pages S201–S217, March 2013; © 2013, Earthquake Engineering Research Institute

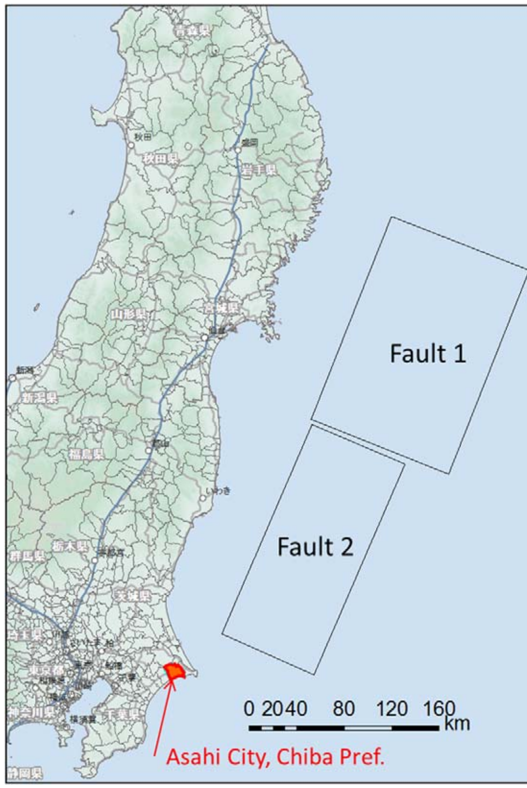

Figure 1. Locations of Asahi City, Chiba Prefecture, and the fault model developed by the Geospatial Information Authority of Japan (GSI).

reported as 229. The damage to buildings was concentrated in the Iioka district in the eastern part of the city. The authors surveyed Asahi City for the first time on March 18, a week following the earthquake. Figure 3 shows the survey route and photographs of damaged buildings. Many damaged buildings were observed along not only the coastline but also a road on the survey route, further away from the coastline.

In this study, tsunami-inundated areas in Asahi City, Chiba Prefecture, were identified on the basis of the map compiled by disaster relief volunteers, the interpretation of satellite images, and a numerical simulation of tsunami propagation. The relationship between the fraction of totally collapsed buildings in Asahi City and the depth of inundation, obtained from the numerical simulation, was developed.

DEVELOPMENT OF GEOGRAPHIC INFORMATION SYSTEM FOR TSUNAMI-INUNDATED AREAS IN ASAHI CITY, CHIBA PREFECTURE

To confirm the areas inundated by the tsunami, the authors visited Asahi City on three occasions and conducted field surveys and interviews. Maps developed by the disaster relief volunteers showing the extent of tsunami inundation were provided by the city government

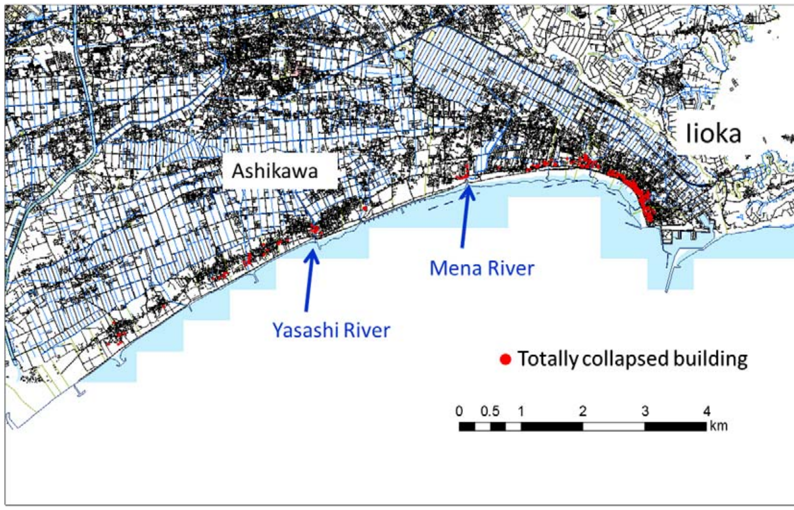

Figure 2. Distribution of totally collapsed buildings after the tsunami in Asahi City, Chiba Prefecture.

Figure 3. Survey route and examples of damaged buildings in Asahi City, Chiba Prefecture.

during the second field survey conducted on 12 April 2011. The tsunami-inundated areas identified by the volunteers were highlighted on regional maps for the city area (Figure 4a). The authors obtained photographs of these maps and constructed polygons showing the tsunami-inundated areas. These were then projected onto a geographic information system

Figure 4. (a) Tsunami-inundated areas identified by disaster relief volunteers in Asahi City and (b) the identified areas projected onto a GIS system.

(GIS) as shown in Figure 4b. The map of this study covers mainly the Iioka district in the eastern part of Asahi City.

Remotely sensed imageries are effective tools for identifying tsunami-inundated areas (Inoue et al. 2007, Kouchi and Yamazaki 2007, Koshimura et al. 2009, Chen et al. 2005). To this end, critical information about the tsunami of March 2011 was obtained from Google Crisis Response (2011). The satellite images of the eastern part of Asahi City, captured by DigitalGlobe on 12 March 2011 were used. The quality of images permitted identification of the tsunami-inundated areas by visual inspection (Figure 5a). The change in color on the ground was mainly used to identify the tsunami-inundated areas. Figure 5b shows the tsunami-inundated areas identified by visual inspection of the satellite images.

The Geospatial Information Authority of Japan (GSI) developed tsunami inundation maps by interpreting satellite and aerial images taken after the earthquake (GSI 2011a). Figure 6 presents a comparison of the tsunami-inundated areas shown in Figures 4 and 5

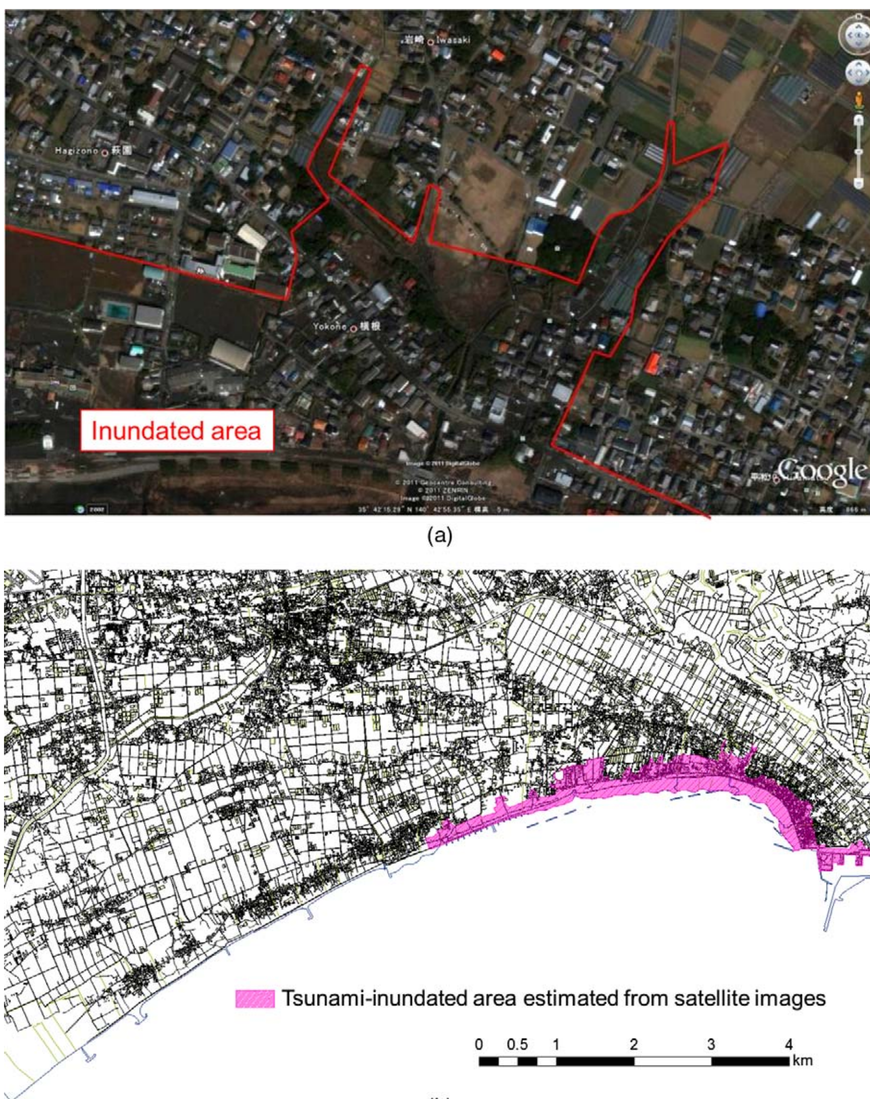

Figure 5. (a) Example of visual inspection of satellite images to identify tsunami-inundated areas and (b) results of the visual analysis in GIS system.

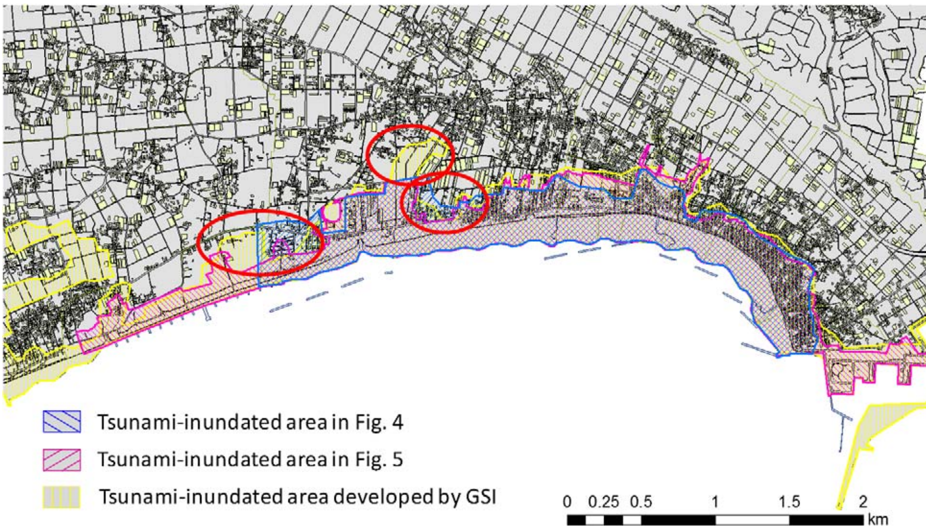

Figure 6. Comparison among the tsunami-inundated areas shown in Figures 4 and 5 and those developed by GSI.

and the results produced by GSI. Overall, the areas of tsunami inundation on the three maps overlapped with one another in the eastern part of Asahi City. The three areas marked with circles indicate sites where the estimates did not coincide. Hence, the authors revisited these sites on 28 June 2011, and interviewed inhabitants to reassess the tsunami-inundated areas. The final estimates of the tsunami-inundated areas are shown in Figure 7. It should be noted that for the western part of Asahi City, only the map developed by GSI was available. The inundated areas in the eastern part could be validated from three different sources: the map drawn by the volunteers, the result of visual inspection of satellite images, and the tsunami inundation map developed by the GSI.

The authors set ten traverse lines in the inundated area and the land elevations along the lines were determined (Figure 8). The GSI digital elevation model with a grid size of 10 m was employed in this study. The results show that the run-up reached a height of approximately 5 m in Asahi City.

Tsunami hazard maps have already been developed for Asahi City (Asahi City 2008) previous to the earthquake. In these maps, the areas of tsunami inundation were estimated on the basis of the past 1677 Empo Boso-oki and the 1703 Genroku Kanto earthquakes (Iwabuchi et al. 2008). Figure 9 shows a comparison of a tsunami hazard map with the identified tsunami-inundated areas of the city after the 2011 Tohoku Earthquake. It can be observed that the eastern parts of the city, such as Iioka, were affected more severely than expected. Seawalls approximately 4 m in height were constructed in Iioka; however, the tsunami waves over topped the walls and flowed into the residential areas.

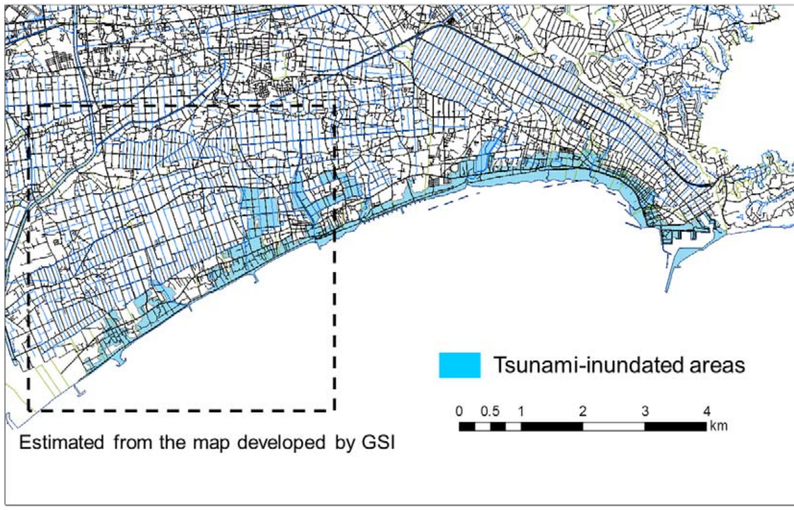

Figure 7. Final estimates of tsunami-inundated areas in Asahi City, Chiba Prefecture, after the 2011 Tohoku-oki earthquake.

Land use and protection structures along the coast were interpreted from satellite images of Google Earth before the tsunami. The images were projected onto the map coordinate system, and the locations of tide-prevention forests and the seawalls were visually identified (Figure 10). It was observed that the tsunami-inundated areas spread mostly along the rivers. In general, the height of tsunami waves exceeded that of the built seawalls. In the areas labeled (*b*) and (*c*), there was comparatively less inundation behind the tide-prevention forests, except for the areas along the rivers. There are both seawalls and tide-prevention forests in the area identified as (*a*), but this region experienced tsunami inundation. The evaluation of the tsunami mitigation strategies that use both natural and artificial approaches has mixed results. As a whole, the integrity of the trees was able to withstand the forces of the tsunami inundation, and there was a density of trees, so that the effects of the tsunami were significantly reduced in several areas. Overall, the ability of tide-prevention forests to reduce tsunami inundation remains somewhat controversial because in the Tohoku district, large areas of coastal forest failed to provide protection (EERI 2011a). In most cases, this was simply because the tsunami force was too large and the trees were destroyed. For Asahi City, Chiba Prefecture studied in this paper, the tsunami forces might be smaller and the trees survived, providing some measure of protection.

NUMERICAL SIMULATION OF TSUNAMI PROPAGATION

Numerical simulation of tsunami propagation was performed to estimate the tsunami-inundated areas in Asahi City. The seismic fault model developed by the GSI (2011b) was employed to estimate the vertical displacement of the seabed (see Figure 1). The specifications of this fault model are listed in Table 1. Figure 11 shows the vertical displacement estimated by Okada's method (Okada 1985). Assuming the water layer to be incompressible, the estimated vertical displacement of the seabed was regarded as the initial profile of the tsunami.

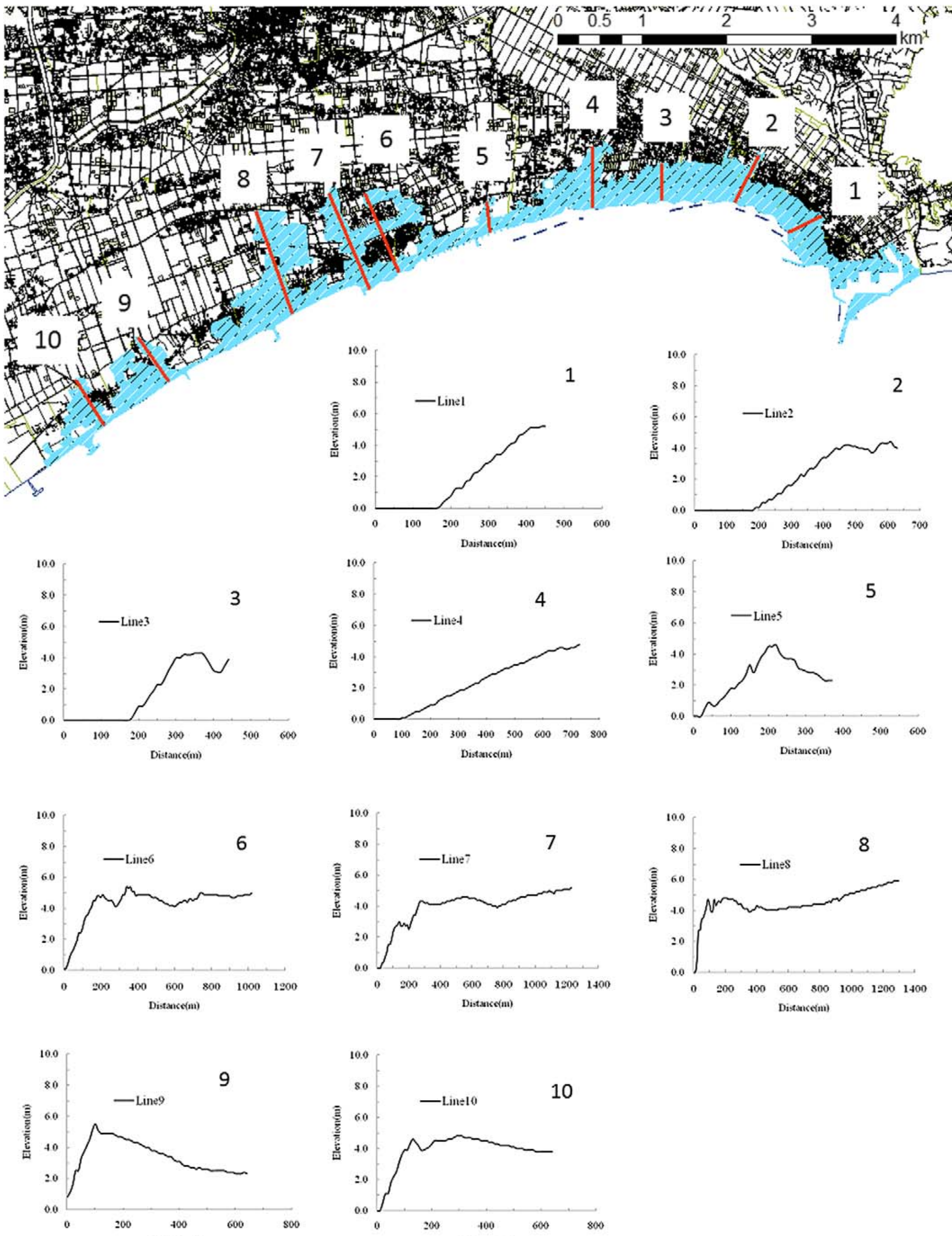

Figure 8. Distribution of land elevations along the transverse lines in the identified tsunami-inundates areas in Asahi City.

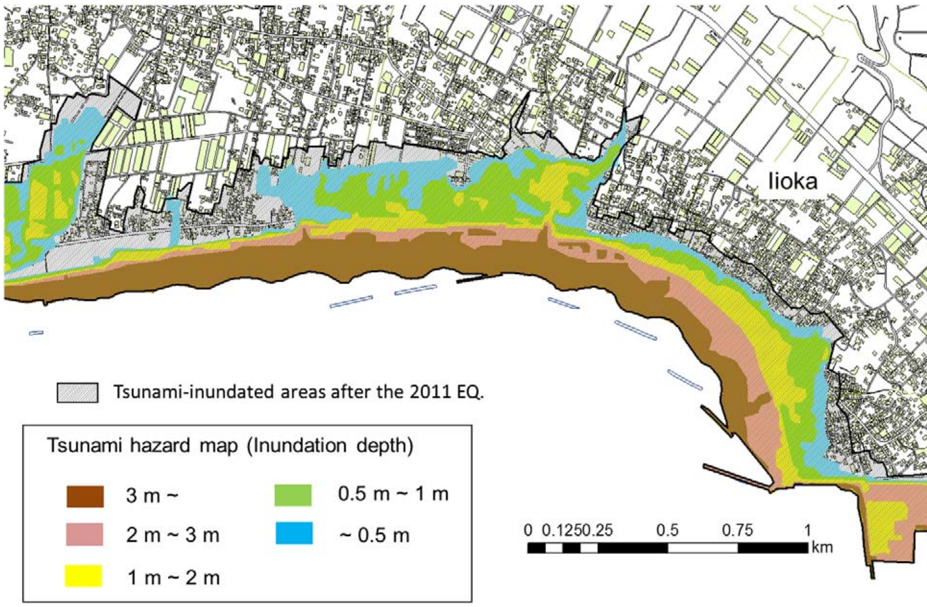

Figure 9. Comparison between tsunami hazard map and identified tsunami-inundated areas in Asahi City, Chiba Prefecture, after the 2011 Tohoku-oki earthquake.

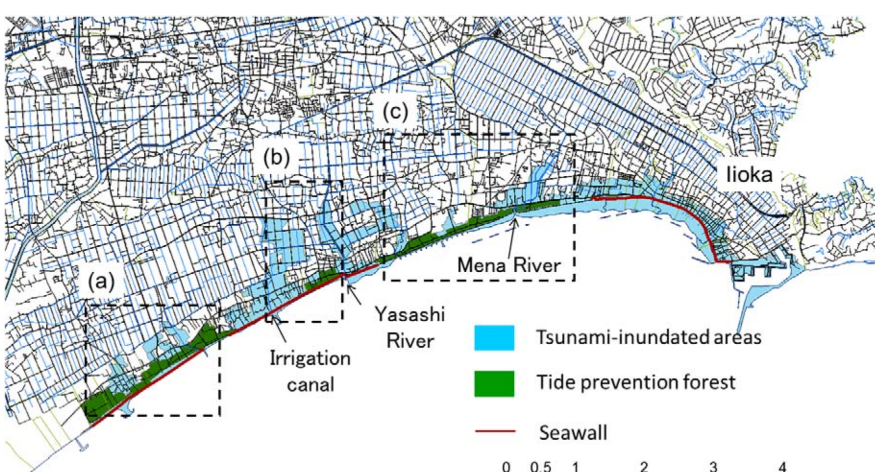

Figure 10. Land use classification along the coastal line and the tsunami-inundated areas in Asahi City.

Table 1. Specifications of the seismic fault model developed by the GSI (2011b)

	Depth (km)	Length (km)	Width (km)	Strike (deg)	Dip (deg)	Rake (deg)	Slip (m)
Fault 1	5.1	186	129	203	16	101	24.7
Fault 2	17.0	194	88	203	15	83	6.1

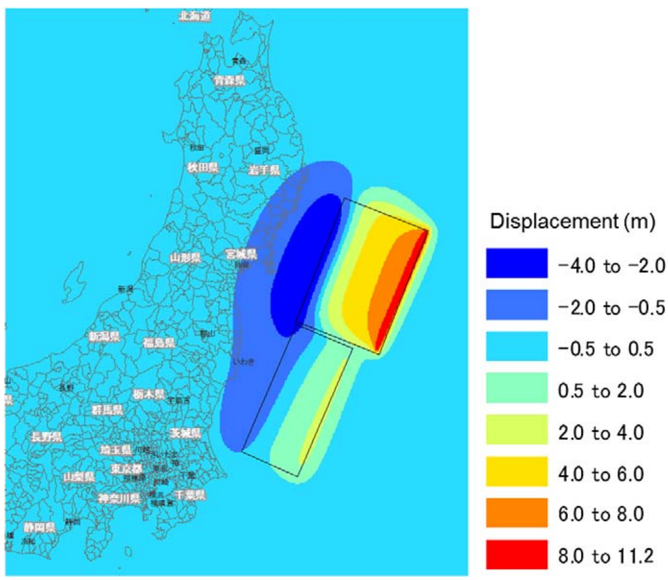

Figure 11. Vertical displacement of seabed as estimated by Okada's method (1985).

Various methodologies have been employed to simulate tsunami propagation (Ohmachi et al. 2001, Furumura and Saito 2009, Liu et al. 2008). In this study, we used TUNAMI-CODE (Imamura 1995) for modeling the tsunami propagation and the resulting coastal inundation. The model employs a set of nonlinear shallow water equations where bottom friction terms are discretized by a leap-frog finite difference scheme. This model is widely used to simulate tsunami propagation and inundation on dry land (Koshimura et al. 2006). Based on the shallow water theory, the continuity equation can be expressed as

$$\frac{\partial \eta}{\partial t} + \frac{\partial M}{\partial x} + \frac{\partial N}{\partial y} = 0 \tag{1}$$

where M and N are the discharge fluxes in the x and y directions, respectively; η is the vertical displacement of the water surface above the still water level. The equations of motion are written as

$$\frac{\partial M}{\partial t} + \frac{\partial}{\partial x}\left(\frac{M^2}{D}\right) + \frac{\partial}{\partial y}\left(\frac{MN}{D}\right) = -gD\frac{\partial \eta}{\partial x} - \frac{gn^2}{D^{7/3}} M\sqrt{M^2 + N^2} \tag{2}$$

$$\frac{\partial N}{\partial t}+\frac{\partial}{\partial x}\left(\frac{MN}{D}\right)+\frac{\partial}{\partial y}\left(\frac{N^2}{D}\right)=-gD\frac{\partial \eta}{\partial y}-\frac{gn^2}{D^{7/3}}N\sqrt{M^2+N^2} \tag{3}$$

where D is the summation of η and the still water depth h and n is Manning's roughness coefficient.

In the numerical simulation, the target region was divided into four sub-regions having grid lengths of 1,350 m, 450 m, 150 m, and 50 m. The sub-regions characterized by coarser grids were set in the deep sea and the ones with finer grids were set closer to shore (Shuto 1991). The h for each grid cell was assigned using the bathymetry data collected by the Japan Coast Guard. The elevations of the land, determined by the GSI were also considered for estimating the inundated areas.

Manning's roughness coefficients were assigned with respect to the land use classifications, as listed in Table 2 (Kotani et al. 1998). We considered that tsunami propagation occurred for three hours after the earthquake. The time step in the numerical simulation was selected to be 0.15 s.

The simulation result was compared with the tidal gauge records. In Chiba Prefecture, a tide station is operated at Choshi fishery port by the Japan Meteorological Agency (JMA). The tide station is located at approximately 13 km east of Iioka port. Figure 12 shows a comparison of the heights of tsunami waves estimated by the numerical simulation with those recorded at the tide station. According to the figure, the estimated maximum height of waves from the model shows good agreement with the recorded data. Moreover, the arrival time of the first tsunami wave calculated in the simulation almost coincides with that observed in the tidal record. However, the total calculated time series does not seem to match the data very accurately. To improve the accuracy, the distribution of vertical displacements of the seabed needs to be obtained for a more detailed fault model, such as determined by the inversion of tsunami wave form (Fujii and Satake 2012).

Figure 13 shows a comparison of the tsunami-inundation depths obtained by the numerical simulation with the tsunami-inundated areas identified in this study. We focus on the eastern part of Asahi City, where the inundated areas were verified through different sources. The simulated distribution of the tsunami-inundated areas and the distribution identified through the surveys show similar trends. The observed tsunami-inundated areas include almost all the surveyed areas with a simulated inundation depth greater than 1 m, but not some of the areas of shallower depth. The observed tsunami-inundated areas were

Table 2. Definition of Manning's roughness coefficient in this study

Land use	Manning's roughness coefficient ($m^{-1/3}s$)
Residential district	0.040
Agricultural land	0.020
Forest land	0.030
Body of water	0.025
Others	0.025

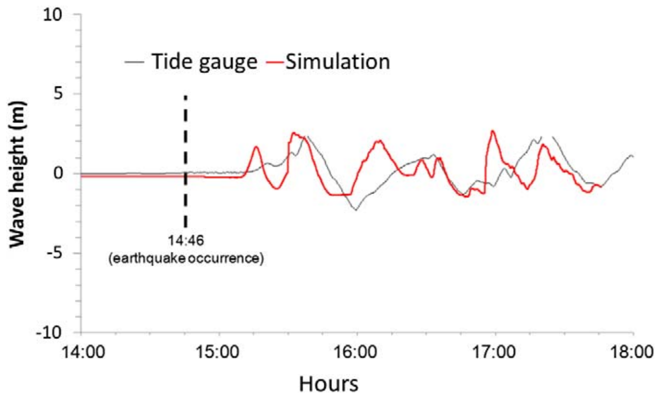

Figure 12. Comparison between the heights of tsunami waves estimated by a numerical simulation and those recorded at Choshi fishery port, Chiba Prefecture.

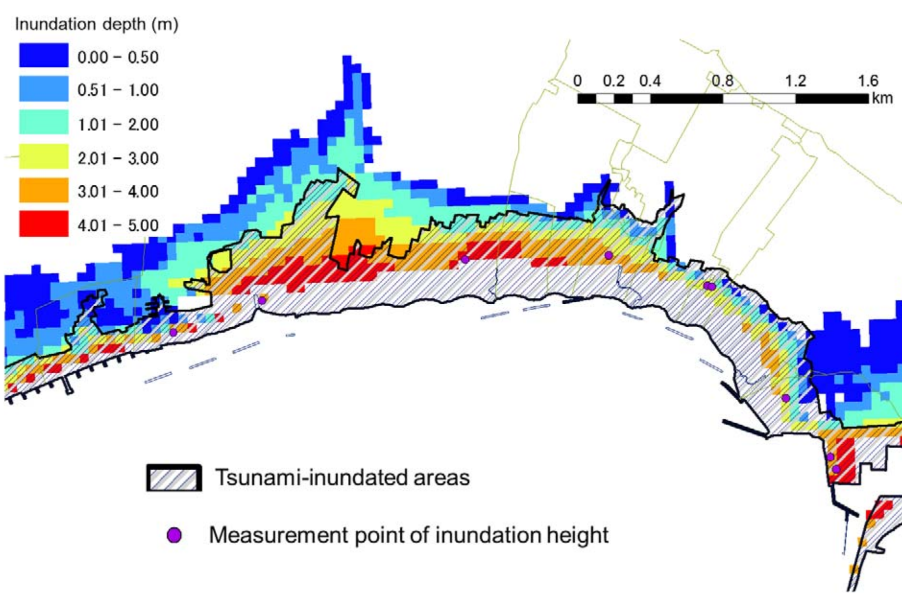

Figure 13. Comparison between inundation depths estimated by a numerical simulation and the actual tsunami-inundated areas identified in this study.

identified primarily through the satellite and aerial images captured a few days after the earthquake. Hence, the areas inundated by shallow waters might have been identified with limited accuracy. This may explain the difference between the inundated areas determined by the simulation and those identified in this study.

The locations of measurement points of tsunami inundation heights along the coastline compiled by the 2011 Tohoku Earthquake Tsunami Joint Survey Group (2011) are also

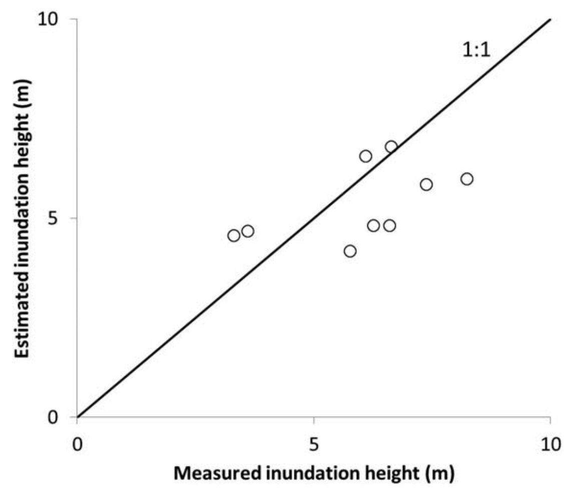

Figure 14. Comparison between the measured tsunami inundation heights and those estimated by a numerical simulation in Asahi City, Chiba Prefecture.

illustrated in Figure 13. The inundation height collected by the survey group is defined as the elevation of water level with reference to the sea level (Tokyo Peil: T.P.) while the tsunami inundation depth shown in Figure 13 is the elevation of water level with respect to the ground level. Figure 14 compares the measured tsunami inundation heights (from the sea level) and those estimated by the numerical simulation. Although the results of the numerical simulation show a reasonable level of agreement with the observations, the estimations of inundation heights tend to be smaller than measured heights at several points. A finer elevation model should be considered in the numerical simulation to improve the accuracy.

The structural performance due to tsunami loading has been investigated by various research teams (Bertero et al. 1985, Saatcioglu 2006, Ruangrassamee et al. 2006). This study tries to obtain the statistics related to structural damage. Because the exact locations of the totally collapsed buildings were available (see Figure 2), a dataset of the actual damage could be established. Then the damage ratio of the buildings—the ratio of totally collapsed buildings to the total number of buildings—in terms of the inundation depth, was evaluated by combining this dataset with the results of the numerical simulation; the resulting data are listed in Table 3. The total number of buildings listed in this table is for tsunami-inundated areas shown in Figure 9. Figure 15 shows the distribution of totally collapsed buildings in the tsunami affected area according to the estimated inundation depths. Building inventories compiled in 2009 by Zenrin, a Japanese map publisher, were used in this study (Zenrin 2012). In this study, we focus on one- and two-story buildings, which are mainly considered to be wooden houses. Figure 16 shows the relationship between the damage ratio of one- and two-story buildings and the estimated tsunami-inundation depths. The figure also shows a fragility curve constructed after the 2004 Sumatra–Andaman earthquake (Koshimura et al. 2009). In the study, pre- and post-event satellite images were employed to perform visual damage inspection. The buildings were interpreted as “survived” or “destroyed” by detecting

Table 3. Damage ratio of one- and two-story buildings with respect to the estimated inundation depth

Inundation depth (m)	Total number of buildings (a)	Number of collapsed buildings (b)	Damage ratio (b/a)
0–0.5	360	11	0.03
0.5–1.0	128	9	0.07
1.0–2.0	254	50	0.20
2.0–3.0	282	78	0.28
3.0–4.0	261	59	0.23
4.0–5.0	108	18	0.17

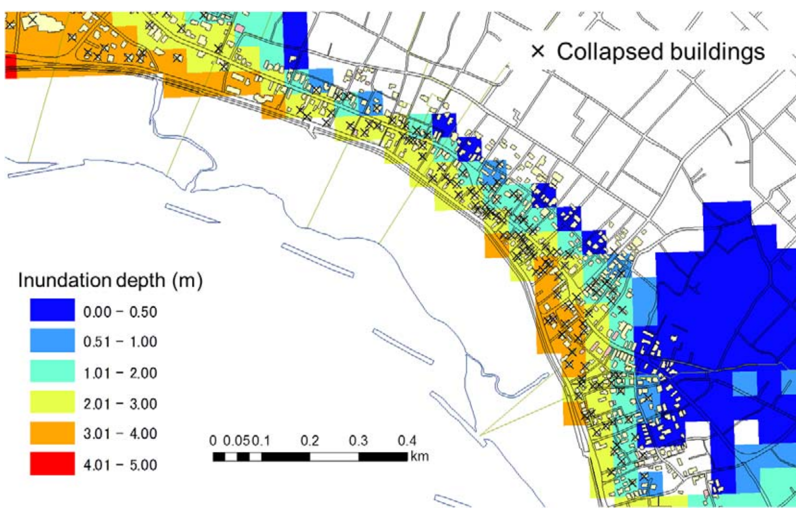

Figure 15. Distribution of totally collapsed buildings according to estimated tsunami-inundation depths.

if the roofs were remained or not, and the fraction of "destroyed" buildings was used as the damage ratio. The damage ratios in Asahi City were similar in level with those in Banda Aceh, Indonesia, for an estimated inundation depth of around 3 m. However, the observed damage ratios in Asahi City associated with the inundation depth of more than 3 m were smaller than the estimations of the fragility function from Indonesia.

In the numerical simulation, a land elevation model with a grid size of 50 m was employed. However, a finer elevation model should be considered to obtain a more accurate result. As mentioned in the description of Figure 12, an improved fault model determined by the inversion analysis of tsunami waveform should be employed in the numerical simulation. To estimate the hydrodynamic forces applied to structures during a tsunami, it is necessary to estimate not only the inundation depth but also the flow velocity that caused the observed

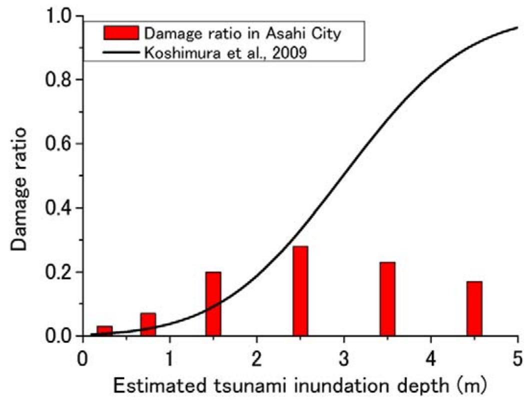

Figure 16. Relationship between the damage ratio of one- and two-story buildings and the estimated tsunami-inundation depth.

damage. This event provided an opportunity to analyze tsunami flow conditions using video and field evidence (EERI 2011b). The damage ratio of buildings in Asahi City, Chiba Prefecture, will be evaluated in terms of the hydrodynamic forces. Furthermore, the structural details of buildings were not considered in evaluating the damage ratios, but these effects should be investigated in a future study. Further research is necessary to provide solid conclusions on the relationship between the damage ratio of buildings and the tsunami inundation depth.

CONCLUSIONS

In this study, the tsunami-inundated areas, associated with the 2011 Tohoku-oki earthquake were estimated for farther distances from the earthquake source in Asahi City, Chiba Prefecture. First, maps drawn by disaster relief volunteers and satellite imageries were employed to identify the tsunami-inundated areas. Then, the propagation of the tsunami was numerically simulated and the simulated inundation areas were compared with the identified areas. Finally, the damage ratio of buildings was evaluated in terms of the estimated tsunami inundation depths.

The GIS dataset for tsunami-inundated areas was constructed by gathering information from different resources and conducting interviews with the residents of the affected areas. It was observed that the tsunami run-up reached a height of approximately 5 m in Asahi City. The 4 m seawalls were not very effective; however, tide-prevention forests may have been effective in providing protection from the tsunami waves in some areas.

A comparison of the simulated and identified tsunami-inundated areas showed that the observed inundated areas cover almost all the areas where the estimated depth was more than 1 m, but not some of the areas of shallower modeled inundations. Since the tsunami-inundated areas were mainly identified based on the satellite images taken a few days after the earthquake, only the areas completely inundated with deep water could be detected. This may explain the difference between the simulated results and those obtained by imagery.

According to the relationship between the damage ratio of buildings and the estimated tsunami inundation depth, the damage ratios associated with the inundation depth of less than 3 m, were consistent with values from Banda Aceh after the 2004 Sumatra–Andaman earthquake. However, the damage ratios for Asahi City were smaller for inundation depths greater than 3 m, compared to the Indonesian data. In order to arrive at more definite conclusions, it is essential to improve the accuracy of the numerical simulation by employing a more detailed fault model and a finer digital-elevation model, and considering the locations of the seawalls.

ACKNOWLEDGMENTS

The authors would like to express their sincere gratitude to Professor Shunichi Koshimura of Tohoku University for providing the TUNAMI-CODE (Tohoku University's Numerical Analysis Model for Investigation of Tsunami). The authors also thank the Japan Meteorological Agency (JMA) for providing the tidal record at Choshi, Chiba Prefecture.

REFERENCES

Asahi City, 2008. http://www.city.asahi.lg.jp/section/soumu/news/2008-0319-1407-2.html (in Japanese).

Asahi City, 2011. http://www.city.asahi.lg.jp/section/soumu/bousai_001.html (in Japanese).

Bertero, V. V., Corley, W. G., Degenkolb, H. J., Hakala, W. W., Hanson, R. D., Jirsa, J. O., Johnston, R. G., Krawinker, H., Lu, L., Mahin, S. A., McClamroch, N. H., Roeder, C. W., Sharpe, R., and Wight, J. K., 1985. Damage survey of the Nihon-Kai-Chubu, Japan, earthquake of May 26, 1983, *Earthquake Spectra* **1**, 319–352.

Cabinet Office, 2011. Outline of Damage due to Tsunami, Government of Japan, available at http://www.bousai.go.jp/jishin/chubou/higashinihon/1/3-2.pdf (in Japanese).

Chen, P., Liew, S. C., and Kwoh, L. K., 2005. Tsunami damage assessment using high-resolution satellite imagery: A case study of Aceh, Indonesia, in *Proceedings of the International Geosciences and Remote Sensing Symposium, IGARSS 2005*, 1405–1408.

Earthquake Engineering Research Institute (EERI), 2011a. *The Japan Tohoku Tsunami of March 11, 2011*, EERI Special Earthquake Report, November 2011.

Earthquake Engineering Research Institute (EERI), 2011b. *The Tohoku, Japan, Tsunami of March 11, 2011: Effects on Structures*, EERI Special Earthquake Report, September 2011.

Fujii, Y., and Satake, K., 2012. Tsunami Source of the Off Tohoku-Pacific Earthquake on March 11, 2011 (Tentative Result, Ver. 4.2 and Ver. 4.6), available at http://iisee.kenken.go.jp/staff/fujii/OffTohokuPacific2011/tsunami_inv.html.

Furumura, T., and Saito, T., 2009. Integrated ground motion and tsunami simulation for the 1944 Tonankai earthquake using high-performance supercomputers, *Journal of Disaster Research* **4**, 118–126.

Geospatial Information Authority of Japan (GSI), 2011a. http://www.gsi.go.jp/kikaku/kikaku40014.html (in Japanese).

Geospatial Information Authority of Japan (GSI), 2011b. http://www.gsi.go.jp/cais/topic110422-index.html (in Japanese).

Google Crisis Response, 2011. Resources related to the 2011 Japan Crisis, http://www.google.com/intl/en/crisisresponse/japanquake2011.html.

Imamura, F., 1995. Review of tsunami simulation with a finite difference method, *Long-Wave Runup Models*, World Scientific, 25–42.

Inoue, S., Wijeyewickrema, A. C., Matsumoto, H., Miura, H., Gunaratna, P., Madurapperuma, M., and Sekiguchi, T., 2007. Field survey of tsunami effects in Sri Lanka due to the Sumatra-Andaman earthquake of December 26, 2004, *Pure and Applied Geophysics* **164**, 395–411.

Iwabuchi, Y., Sugino, H., Ebisawa, K., and Imamura, F., 2008. Reviewed database of the tsunami Run-up Data on the Documentation in Japan, in *Proceedings of the 14th World Conference on Earthquake Engineering*, Paper ID 15-0036, p. 8.

Koshimura, S., Katada, T., Mofjeld, H. O., and Kawata, Y., 2006. A method for estimating casualties due to the tsunami inundation flow, *Natural Hazards* **39**, 265–274.

Koshimura, S., Matsuoka, M., and Kayaba, S., 2009. Integrated approach to assess the impact of tsunami disaster, in *Proceedings of ICOSSAR 2009*, 2302–2307.

Koshimura, S., Oie, T., Yanagisawa, H., and Imamura, F., 2009. Developing fragility functions for tsunami damage estimation using numerical model and post-tsunami data from Banda Aceh, Indonesia, *Coastal Engineering Journal*, JSCE, **51**, 243–273.

Kotani, M., Imamura, F., and Shuto, N., 1998. New method of tsunami runup and estimation of damage using GIS data, in *Proceedings of the Coastal Engineering*, JSCE, **45**, 356–360 (in Japanese).

Kouchi, K., and Yamazaki, F., 2007. Characteristics of tsunami-affected areas in moderate-resolution satellite images, *IEEE Transactions on Geoscience and Remote Sensing* **45**, 1650–1657.

Liu, P. L. F., Yeh, H., and Synolakis, C., 2008. Advanced numerical models for simulating tsunami wave and runup, *Advances in Coastal and Ocean Engineering*, World Scientific.

National Police Agency of Japan, 2011. Damage situation and police countermeasures associated with 2011Tohoku district—off the Pacific Ocean Earthquake, available at http://www.npa.go.jp/archive/keibi/biki/higaijokyo_e.pdf.

Ohmachi, T., Tsukiyama, H., and Matsumoto, H., 2001. Simulation of tsunami-induced by dynamic displacement of seabed due to seismic faulting, *Bulletin of the Seismological Society of America* **91**, 1898–1909.

Okada, Y., 1985. Surface deformation due to shear and tensile faults in a half-space, *Bulletin of the Seismological Society of America*, **75**, 1135–1154.

Ruangrassamee, A., Yanagisawa, H., Foytong, P., Lukkunaprasit, P., Koshimura, S., and Imamura, F., 2006. Investigation of tsunami-induced damage and fragility of buildings in Thailand after the December 2004 Indian Ocean tsunami, *Earthquake Spectra* **22**, S377–S401.

Saatcioglu, M., Ghobarah, A., and Nistora, I., 2006. Performance of structures in Thailand during the December 2004 Great Sumatra earthquake and Indian Ocean tsunami, *Earthquake Spectra* **22**, S355–S375.

Shuto, N., 1991. Numerical simulation of tsunamis—Its present and near future, *Natural Hazards* **4**, 171–191.

The 2011 Tohoku Earthquake Tsunami Joint Survey Group, 2011. Nationwide field survey of the 2011 off the Pacific Coast of Tohoku Earthquake tsunami, *Journal of Japan Society of Civil Engineers*, Ser. B2 (Coastal Engineering), **67**, 63–66.

Zenrin, 2012. http://www.zenrin.co.jp/english/index.html.

(Received 30 March 2012; accepted 26 November 2012)